NASA TECHNICAL NOTE

NASA TN D-7212

NASA TN D-7212



# AFTERBURNER PERFORMANCE OF CIRCULAR V-GUTTERS AND A SECTOR OF PARALLEL V-GUTTERS FOR A RANGE OF INLET TEMPERATURES TO 1255 K (1800° F)

*by J. Robert Branstetter and Gregory M. Reck*

*Lewis Research Center*
*Cleveland, Ohio 44135*

NATIONAL AERONAUTICS AND SPACE ADMINISTRATION • WASHINGTON, D. C. • MARCH 1973

| 1. Report No. | 2. Government Accession No. | 3. Recipient's Catalog No. |
|---|---|---|
| NASA TN D-7212 | | |

| 4. Title and Subtitle | 5. Report Date |
|---|---|
| AFTERBURNER PERFORMANCE OF CIRCULAR V-GUTTERS AND A SECTOR OF PARALLEL V-GUTTERS FOR A RANGE OF INLET TEMPERATURES TO 1255 K (1800° F) | March 1973 |
| | 6. Performing Organization Code |

| 7. Author(s) | 8. Performing Organization Report No. |
|---|---|
| J. Robert Branstetter and Gregory M. Reck | E-7262 |
| | 10. Work Unit No. 501-24 |

| 9. Performing Organization Name and Address | 11. Contract or Grant No. |
|---|---|
| Lewis Research Center<br>National Aeronautics and Space Administration<br>Cleveland, Ohio 44135 | |

| 12. Sponsoring Agency Name and Address | 13. Type of Report and Period Covered |
|---|---|
| National Aeronautics and Space Administration<br>Washington, D. C. 20546 | Technical Note |
| | 14. Sponsoring Agency Code |

15. Supplementary Notes

16. Abstract

Combustion tests of two V-gutter types were conducted in a 49-centimeter (19.25-in.) diameter duct using vitiated air. Fuel spraybars were mounted in line with the V-gutters. Combustor length was set by flame-quench water sprays which were part of a calorimeter for measuring combustion efficiency. Although the levels of performance of the parallel and circular array afterburners were different, the trends with geometry variations were consistent. Therefore, parallel arrays can be used for evaluating V-gutter geometry effects on combustion performance. For both arrays, the highest inlet temperature produced combustion efficiencies near 100 percent. A 12.7-centimeter (5-in.) spraybar - to - V-gutter spacing gave higher efficiency and better lean blowout performance than a spacing twice as large. Gutter durability was good.

| 17. Key Words (Suggested by Author(s)) | 18. Distribution Statement |
|---|---|
| Afterburner; V-gutter; Flameholder; Thrust augmentation; Combustion efficiency; Combustor test facility | Unclassified - unlimited |

| 19. Security Classif. (of this report) | 20. Security Classif. (of this page) | 21. No. of Pages | 22. Price* |
|---|---|---|---|
| Unclassified | Unclassified | 39 | $3.00 |

* For sale by the National Technical Information Service, Springfield, Virginia 22151

# AFTERBURNER PERFORMANCE OF CIRCULAR V-GUTTERS AND A SECTOR OF PARALLEL V-GUTTERS FOR A RANGE OF INLET TEMPERATURES TO 1255 K (1800° F)

by J. Robert Branstetter and Gregory M. Reck

Lewis Research Center

## SUMMARY

Combustion tests were conducted in a 49-centimeter (19.25-in.) diameter duct to compare the performance of a two-ring, circular V-gutter afterburner and a configuration of three, straight, parallel V-gutters. This latter configuration simulated a sector of a much larger afterburner containing circular arrays. All V-gutters were 3.8 centimeters (1.5 in.) wide. ASTM A-1 fuel was injected normal to the airflow from spraybars mounted in line with the gutters. Spraybar - to - V-gutter spacings of 12.7 and 25.4 centimeters (5 and 10 in.) were tested. Combustor length was established at 92 centimeters (36 in.) by a set of water sprays. Vitiated air entered the combustor at temperatures of 920, 1090, or 1255 K (1200°, 1500°, or 1800° F). Inlet pressure and velocity were maintained at 1 atmosphere and 150 meters per second (500 ft/sec), respectively. A fuel-air ratio span of 0.008 to 0.065 was investigated.

The circular array, because of its larger blocked area, produced higher combustion efficiencies but poorer lean blowout performance than did the parallel gutters. Although the level of performance of the parallel and circular array afterburners investigated was different, the trends with geometry variation were consistent. Therefore, parallel arrays can be used for evaluating V-gutter geometry effects on combustion performance.

The two V-gutter arrays provided the following results: Combustion efficiency increased as the inlet temperature was increased. For an inlet temperature of 1255 K (1800° F), the efficiency was near 100 percent. Highest combustion efficiency and best lean blowout results were obtained with the 12.7-centimeter (5-in.) spacing between the fuel injectors (spraybars) and the flameholders (V-gutters). The lean blowout fuel-air ratio appeared insensitive to changes in the inlet temperature but decreased noticeably for a decrease in injector-to-flameholder spacing. Also included are results showing that both combustion efficiency and blowout were insensitive to a change of inlet velocity profile. No gutter damage was observed. The fuel spraybars were subject to clogging at very low fuel flow rates at an inlet temperature of 1255 K (1800° F). The calorimetric apparatus and operating procedure for obtaining combustion efficiency are described.

## INTRODUCTION

This study was undertaken to compare parallel and circular flameholder arrays by evaluating combustion performance and hardware durability at three inlet temperatures. The comparison includes an examination of the effect of fuel mixing distance and inlet velocity profile.

Several years ago, afterburner combustor studies were resumed at Lewis after a lapse of about 10 years (ref. 1). These new studies were prompted by an interest in afterburner operation over an extended range of fuel-air ratios and a trend toward higher turbine discharge temperatures (ref. 2). Operation over an extended range of fuel-air ratios creates combustion efficiency problems. High inlet temperatures aggravate liner cooling problems. Prior work on afterburners is reported in reference 1. This work included an evaluation of straight, parallel burner configurations. Because of facility limitations, inlet temperatures were limited to 920 K (1200$^{\circ}$ F).

In order to conduct combustion tests in the environment required by present-day needs, the reference 1 apparatus was upgraded to provide inlet temperature capabilities to 1255 K (1800$^{\circ}$ F) and variable combustor length. The present study compares parallel and conventional circular V-gutter arrays by evaluating combustion performance and hardware durability using vitiated air at inlet temperatures of 920, 1090, and 1255 K (1200$^{\circ}$, 1500$^{\circ}$, and 1800$^{\circ}$ F). The study places emphasis on combustion efficiency and on operating range as indicated by lean blowout limits. A 49-centimeter (19.25-in.) diameter duct was used to test a two-ring V-gutter afterburner and a configuration of three, straight, parallel V-gutters. This latter configuration simulated a sector of a larger diameter circular array. Combustor length was established at 92 centimeters (36 in.) by a set of water sprays. Inlet pressure and velocity were maintained at 1 atmosphere and 150 meters per second (500 ft/sec), respectively. A fuel-air ratio span of 0.008 to 0.065 was investigated.

## COMBUSTION PERFORMANCE CONSIDERATIONS

The concept of parallel flameholder arrangement within the confines of a relatively small-diameter duct (ref. 1) had been found to provide good flexibility of hardware arrangement. Scaling problems had appeared minimal in that there appeared to be no physical scaling of pertinent dimensions affecting the complex kinetic processes of mixture preparation and combustion. Dimensions considered most critical were afterburner length, flameholder width and lateral spacing, and fuel-injector-to-flameholder longitudinal spacing.

For the present investigation simple V-gutters and fuel spraybars were selected

because they are the best-understood types. To minimize the adverse effect of flame quenching at the duct wall, spraying of fuel in the vicinity of the walls was kept to a minimum. The longitudinal distances between fuel spraybars and V-gutters were chosen to provide stable combustion at intermediate values of thrust augmentation, that is, at fuel-air ratios near one-half stoichiometric values. An examination of reference 3 blowout correlation results had shown that longer mixing distances would produce premature lean blowouts. To obtain the maximum possible uniformity of fuel distribution in the flame recirculation zone immediately downstream of the V-gutter, small and closely spaced fuel orifices were used. Flame uniformity should aid the interpretation of blowout results. Afterburner length was chosen to provide a spread in the combustion efficiency values and thereby ease the task of interpreting the combustion efficiency results.

For the present inlet conditions, inlet pressure and inlet velocity are expected to be subordinate to inlet temperature as factors affecting combustion efficiency level (ref. 3). However, in recognition of the wide variety of velocity profiles encountered in practice, two profiles were studied.

Combustor hardware materials were selected on the basis of strength and oxidation resistance at elevated temperatures.

# APPARATUS

## Test Facility

A diagram of the test facility is presented in figure 1. The combustion air was heated in a tube-type heat exchanger and metered with an orifice. A choked butterfly valve located downstream regulated the flow and a perforated cylinder dispersed the air into the inlet plenum. After passing through the vitiating preheater and test section, the afterburner exhaust was quenched and calorimetrically measured. Finally, the gases were further quenched and exited through an exhaust butterfly valve into the altitude exhaust system.

The test apparatus was contained within a safety shroud, as shown in figure 1. The shroud guided purge air around the test apparatus, thereby reducing the possibility of fuel accumulation in the event of a leak.

ASTM A-1 kerosene was supplied to the afterburner through a conventional system containing flowmeters, a throttle valve, and a positive shutoff valve. Another fuel system provided gasoline to the vitiating preheater.

## Test Apparatus

The vitiating preheater, afterburner, and enthalpy balance sections are shown schematically in figure 2. The vitiating preheater consisted of four J-57 combustor cans (fig. 3) mounted on a bulkhead. A mixing section (fig. 4) was located at the aft end of each combustor can. Each mixer consisted of two concentric shells bolted to the downstream side of the bulkhead.

Pertinent details of the afterburner test section are shown in figure 5. Two inlet velocity profiles - a "flat" and a "lobed" - were investigated. The baffle in figure 5 was used for the flat profile tests. An internal flow of air cooled the baffle. The water spray head is shown in figure 6. The spray head could be positioned at any axial location within the combustion chamber. Sprays were directed normal to the gas flow. Each of the two rings of figure 6 was supplied with its own flow system. A third set of metered water sprays located at the plane of casing-diameter enlargement (fig. 5) was used when needed to assist in cooling the enthalpy balance casing. Vanes and wall-mounted baffles in the enthalpy balance section (fig. 2) promoted mixing and vaporization of the quench water.

The combustion chamber length, defined as the distance from the downstream face of the V-gutters to the flame-quench plane, was set at 92 centimeters (36 in.). Chamber diameter was 49.0 centimeters (19.25 in.). The resulting reference area was 1878 square centimeters (291 sq in.).

## Afterburner Designs

Two V-gutter configurations, a circular design and a straight parallel design, were investigated and are shown in figures 7 and 8, respectively. Each array was coplanar. The gutters and support hardware were made from cobalt-base sheet. The projected area of the parallel gutters blocked 21.6 percent of the reference area. The circular gutters blocked 30.8 percent of the reference area. All gutters had a width of 3.8 centimeters (1.5 in.). The fuel bars were made from nickel-base alloy. Hole diameter was 0.05 centimeter (0.02 in.) and injection was normal to the gas flow. The bars were mounted in a fixed position that was either 12.7 or 25.4 centimeters (5 or 10 in.) upstream of the flameholder trailing edge. This spacing was varied by varying the length of the V-gutter support straps. The fuel injectors were connected to a common manifold.

## Instrumentation

Airflow rate was measured by a sharp-edged orifice with flange pressure taps installed according to ASME specifications. The location of other fixed-position pressure and temperature sensors is shown in figure 9. Dynamic pressure transducers were flush mounted on the flow straightening section with diaphragms exposed to the gas flow in order to detect the presence of acoustic resonance (screech). The outputs of these transducers were displayed in the control room and were recorded on a high-speed oscillograph.

Two turbine-type flowmeters were series mounted in the ASTM A-1 supply system and also in the gasoline supply system for the direct-fired preheater. Three turbine-type flowmeters were mounted in the flame-quench water system - one measuring the total flow rate, and one in each of the two parallel systems delivering the water to the quench spraybars. The cooling water for the afterburner combustion sections (fig. 2) was supplied by two independent sources, each of which contained a throttle valve and a flow measuring device.

Data from the steady-state instrumentation were recorded by the laboratory's automatic data recording and processing system (refs. 4 and 5). A portion of the instrumentation was connected to an analog computer which provided a continuous display in the control room of airflow rate and fuel-air ratio.

## TEST PROCEDURE

The following three afterburner-inlet test conditions were investigated:

| | Test condition | | |
|---|---|---|---|
| | A | B | C |
| Total temperature, K ($^{o}$F) | 920 (1200) | 1090 (1500) | 1255 (1800) |
| Static pressure, N/cm$^2$ (psia) | 10.0 (14.5) | 10.0 (14.5) | 10.0 (14.5) |
| Velocity, m/sec (ft/sec) | 150 (500) | 150 (500) | 150 (500) |
| Preheater-inlet total temperature, K ($^{o}$F) | 450 (350) | 450 (350) | 450 (350) |
| Nominal airflow rate, kg/sec (lb/sec) | 11 (25) | 9 (20) | 8 (18) |
| Nominal preheater fuel-air ratio | 0.012 | 0.017 | 0.022 |

Afterburner ignition was initiated for test conditions A and B. Ignition was accomplished by momentarily increasing the fuel flow to the vitiating preheater and torching to the V-gutters. Performance data were taken over as wide a range of fuel-air ratios as was possible without exceeding stoichiometric mixture. Lean blowout points were determined by slowly decreasing afterburner fuel flow until flameout occurred. Blowout was detected by a decrease in combustor pressure and/or temperature at the enthalpy balance exit plane. A borescope and gutter-mounted thermocouples assisted blowout detection. The blowout point defined the lowest value of fuel-air ratio that could sustain a flame in the shelter of the flameholder. Usually, this fuel-air ratio was first detected by a sudden drop of approximately 5 percent in chamber pressure. The first gutter to blow out defined the blowout fuel-air ratio. Test condition C required a special procedure since fuel decomposition and subsequent spraybar clogging were encountered at fuel-air ratios less than 0.010. The clogging problem was circumvented by igniting the afterburner at test condition A or B, prior to shifting to condition C. Lean blowout tests could not be attempted at test condition C.

In several instances, the upper limit of fuel-air ratio was fixed by the onset of combustion resonance. At test condition A, the upper limit was a result of thermal choking in the enthalpy balance section.

Combustion efficiency was obtained by using an enthalpy balance technique which required that no liquid water be present at the enthalpy balance plane. To ensure this, the average gas temperature at the enthalpy balance plane was maintained at 700 K ($800^{\circ}$ F) or greater by controlling the quench-water flow rate. Data used for computation of combustion efficiency were obtained only after the system reached thermal equilibrium.

## CALCULATIONS

### Afterburner Fuel-Air Ratio (Unburned)

To include the effects of vitiation of the inlet air and incomplete combustion in the preheater, the afterburner fuel-air ratio (unburned) was computed by dividing the total fuel flow available to the afterburner by the available unburned airflow. All data are presented in terms of this fuel-air ratio. Further discussion is included in appendix A.

### Velocity and Mach Number

Inlet velocity and inlet Mach number were calculated from the measured airflow

rate, the inlet reference area of the afterburner test section, the average inlet total temperature, and the inlet static pressure. Lip velocity was calculated as the product of inlet velocity and the term (100/(100 - area blockage, percent)).

## Combustion Efficiency

Combustion efficiency was defined as the ratio of the heat output of the afterburner to the chemical energy of all fuel entering the afterburner. The combustion efficiency equation and its derivation are included in appendix A. Heat-transfer losses from the duct components and the vitiating effect of the direct-fired preheater were included in the calculations. The heat-transfer losses consisted of measured losses from the water-cooled sections and small estimated radiation losses from the enthalpy balance section. The sum of all heat-transfer losses amounted to 23 to 70 joules per gram of air (10 to 30 Btu/lb of air). The value of afterburner inlet temperature ($T_{in}$ of appendix A) used in the calculation of afterburner combustion efficiency was computed from the preheater inlet-air temperature, the preheater fuel-air ratio, and the preheater combustion efficiency. This procedure was necessary since the technique of torching the preheater for afterburner ignition sometimes damaged the afterburner inlet thermocouples.

## Accuracy of Combustion Efficiency Data

Details of the operating characteristics of the calorimeter are given in appendix B. An error analysis is presented in appendix C, along with a discussion of the influence that dissociated combustion products have on the computed value of combustion efficiency. Because of the dissociation, the efficiency values are very likely too low at fuel-air ratios larger than 0.04.

# RESULTS AND DISCUSSION

## Comparison of Circular and Parallel V-Gutter Geometries

General. - The following comparisons discuss the practicality of using parallel V-gutter arrays in place of circular V-gutter arrays to facilitate testing. Comparisons are made on the basis of combustion efficiency, blowout, and durability. Combustion efficiency and blowout data obtained with the circular V-gutters and with the parallel

V-gutters for three test conditions are presented in figures 10 and 11, respectively. Data for two spraybar - to - V-gutter spacings are presented. These data were obtained with lobed inlet velocity profiles which had a local high-velocity core 30 percent above the average. A lobed profile was used to simulate profiles encountered by afterburners in actual engine application. Typical examples of the inlet velocity profile and the inlet temperature profile are presented in appendix B.

For purposes of comparison, the data curves of figures 10 and 11 have been replotted in figure 12. Certain critical dimensional differences which influence the comparison are as follows: Lateral spacing of the circular V-gutters was 8.9 centimeters (3.5 in.). Spacing of the parallel gutters was 12.7 centimeters (5 in.). The projected blocked area of the circular gutters was approximately 40 percent greater than the blockage provided by the parallel gutters. Thus, flow velocity past the lip of the flameholder was 220 and 195 meters per second (720 and 635 ft/sec) for the circular and parallel arrays, respectively.

Combustion efficiency. - Combustion efficiency values used for comparing the two V-gutter configurations were taken at a fuel-air ratio of 0.03. This fuel-air ratio represents an intermediate thrust augmentation value and is a typical design value for many afterburner applications. Also, at 0.03 the data curves are reasonably flat and instrumentation errors are at a minimum, as described in appendix C.

As shown in figure 12, the circular geometry produced higher combustion efficiency values than the parallel V-gutter array. At 0.03 fuel-air ratio, the maximum efficiency difference is 6 percent and occurs in figure 12(b) at an inlet temperature of 920 K ($1200^{\circ}$ F). Figure 12 data show that the efficiency differences between the two arrays is 0 to 3 percent for inlet temperatures of 1090 and 1255 K ($1500^{\circ}$ and $1800^{\circ}$ F), and 2 to 6 percent for an inlet temperature of 920 K ($1200^{\circ}$ F).

A likely cause for the higher combustion efficiency of the circular array stems from flame kinetics. The rate of flame spreading across the flame surfaces combined with the lateral distance the flame must travel can be expected to establish the overall chemical conversion rate discussed in reference 6. At the two higher inlet temperatures, flame spreading is sufficiently rapid that the differences in lateral spacing between the two gutter arrays produces only a small effect on combustion efficiency. At the lowest inlet temperature, flame spreading is slower and the observed efficiency differences are more pronounced.

Blowout. - Overall blowout results of figure 12 show that the parallel array had better blowout characteristics than the circular array. Only at an inlet temperature of 920 K ($1200^{\circ}$ F) is the lean blowout limit for the circular gutters as low as the lean blowout limit for the parallel array. This result is not surprising since the circular array, because of its higher blockage, produced higher lip velocities past the flameholder.

Generally, differences in blowout values for the two V-gutter arrays were marginal and may be insignificant when the lip velocity differences and complexity of obtaining

meaningful data are considered. Selection of a blowout fuel-air ratio was often difficult. Sometimes one local area of sheltered flame would persist at very low fuel-air ratios. Also, failure of flame to spread laterally from a gutter was occasionally misconstrued to be blowout. The inability of a flame to spread is described on page 135 of reference 7. Poor flame spreading is the likely cause of the pronounced change in slope of some data curves of figures 10 and 11 in the vicinity of the blowout point.

Durability. - Durability differences between the two types of arrays were not detected. Visual inspection of the gutters showed no warpage or other signs of deterioration. Gutter temperatures, typified by the data of figure 13 were of similar magnitude for the two arrays. These data were obtained concurrently with the performance data by thermocouples distributed on the metal surfaces.

Fuel tube clogging presented problems with 1255 K (1800° F) inlet temperature. Fuel overheating was sufficiently great at low fuel flow rates that fuel orifices sometimes fouled. In such cases, performance data were discarded. Clogging, as evidenced by injection pressure data, did not occur at intermediate fuel-air ratios.

## Effect of Inlet Temperature and Fuel Mixing Distance on Blowout and Combustion Efficiency

Blowout. - As shown in figures 10 and 11, the lean blowout fuel-air ratio appeared somewhat insensitive to changes in the inlet temperature. Increasing inlet temperature from 920 to 1255 K (1200° to 1800° F) had no discernible influence on the lean blowout limit for the circular array. Although blowout literature does not fully explain the insensitivity of lean blowout limit to large changes in inlet temperature, an afterburner blowout correlation (ref. 3) does show only small lean-limit changes in fuel-air ratio for the range of inlet temperatures of the present investigation. For example, the reference 3 blowout prediction would be 0.03 for an inlet temperature of 920 K (1200° F) and 0.027 for an inlet temperature of 1255 K (1800° F). (The referenced correlation was based on a uniform, premixed, vaporized fuel-air mixture at entry into the flameholder plane.)

Blowout occurred at lower values of fuel-air ratio for the closely spaced injector-flameholder combinations than for the larger spacings. The blowout fuel-air ratio for the circular arrays increased from a value of 0.012 for the small spacing to a value of 0.018 for the large spacing. While the amount of blowout data for the parallel V-gutters was minimal, lean blowout fuel-air ratios were similarly lowered by decreasing spacing (fig. 11).

Combustion efficiency. - Effects of inlet temperature and fuel mixing distance on combustion are shown in figure 14. These data are for parallel arrays and are replots

of figure 11. Results for circular arrays also show the same trends. Combustion efficiency increased as the inlet temperature was increased from 920 to 1255 K (1200° to 1800° F). Near the 1255 K (1800° F) value, efficiency was near 100 percent and was insensitive to changes in the inlet temperature value. For the three fuel-air ratios examined, the smaller spacing always yielded the higher efficiency value. Efficiency differences, resulting from spacing changes, were greatest at a fuel-air ratio of 0.02 and progressively decreased as the fuel-air ratio increased.

## Effect of Inlet Velocity Profile on Performance

For engines, the afterburner inlet velocity profiles become distorted within the diffuser. The extent by which a velocity profile change would influence the previous comparisons may be inferred by examining circular v-gutter performance for both lobed and flat profiles. Performance results for a flat velocity profile are presented in figure 15. The data of figures 10 and 15 are replotted in figure 16. Figure 16 shows the effect of profile shape on combustion efficiency to be inconsequential. Combustion efficiency differences are usually less than 2 percent, and the maximum efficiency values differ by no more than 2 percent. Overall, the maximum efficiency difference is 4 percent and occurs at the highest inlet temperature and at a fuel-air ratio of 0.05. In this region, however, data error is of comparable magnitude.

All blowouts with the 12.7-centimeter (5-in.) spacing, shown in figure 16(a), occurred near a fuel-air ratio of 0.012. With the larger injector-to-flameholder spacing (fig. 16(b)), blowout generally shifted to a value of 0.018. The largest effect of profile on blowout occurs with the larger spacing, where the flat profile produced a very lean, unaccounted-for blowout (fig. 16(b)).

The lobed profile, with its high-velocity core, was expected to produce blowout on the inner gutter. To the contrary, blowouts at an inlet temperature of 920 K (1200° F) for both profiles occurred on the outer gutter. Possibly the high-velocity core kept the fuel from spreading laterally, thereby concentrating fuel on the inner gutter. At an inlet temperature of 1090 K (1500° F), blowouts did occur on the inner gutter.

In summary, only very small effects on combustion performance could be detected for the two inlet velocity profiles.

## SUMMARY OF RESULTS

Performance of two types of afterburner arrays, a parallel and a circular design, were tested at inlet temperatures of 920, 1090, and 1255 K (1200°, 1500°, and 1800° F). Also examined were fuel-spraybar - to - V-gutter spacings of 12.7 and 25.4 centimeters

(5 and 10 in.). Inlet velocity and pressure were 150 meters per second (500 ft/sec) and 1 atmosphere, respectively. Combustor length was fixed at 92 centimeters (36 in.) and gutter width was 3.8 centimeters (1.5 in.). A fuel-air ratio span of 0.008 to 0.065 was investigated. The results were as follows:

1. The applicability of using parallel arrays to represent circular arrays was demonstrated by the following results which apply equally to both arrays:

a. Combustion efficiency increased as afterburner inlet temperature increased. In the vicinity of 1255 K (1800° F) the efficiency was near 100 percent and was insensitive to changes in the inlet temperature value.

b. The smaller of the two injector-to-flameholder spacings always yielded the higher combustion efficiency values at fuel-air ratios to 0.04. Efficiency differences, as a result of spacing, were greatest in the vicinity of a fuel-air ratio of 0.02. These differences decreased as the fuel-air ratio was increased.

c. Lean blowout fuel-air ratio appeared insensitive to changes of inlet temperature.

d. Lean blowout fuel-air ratio decreased noticeably for a decrease in injector-to-flameholder spacing.

e. Durability was good. There was no observed gutter damage. At the highest inlet temperature, both the circular and parallel spraybars were subject to clogging at very low fuel-flow rates.

2. The circular arrays provided higher combustion efficiency than did the parallel arrays. At the two higher inlet temperatures the difference was usually 0 to 3 percent. At the lowest inlet temperature the difference was usually 2 to 6 percent. These differences were attributed to the smaller lateral spacing of the circular arrays (greater projected blocked area).

3. The parallel arrays generally provided leaner blowout fuel-air ratios than did the circular arrays. This was attributed to the greater area blockage of the circular arrays, which produced higher flameholder lip velocities.

4. Except for the problem of fuel injector overheating, the afterburner accommodated inlet temperatures of 1255 K (1800° F) without difficulty. Also, performance as measured was found insensitive to rather wide excursions of inlet velocity profile.

Lewis Research Center,
National Aeronautics and Space Administration,
Cleveland, Ohio, January 3, 1973,
501-24.

# APPENDIX A

## CALCULATION OF FUEL-AIR RATIO AND COMBUSTION EFFICIENCY

This appendix, except for minor changes, was obtained from reference 1. The preheater fuel-air ratio $f_{ph}$ and the afterburner fuel-air ratio $f_{ab}$ are calculated by dividing the respective fuel-flow rate by the total airflow rate.

This afterburner fuel-air ratio (unburned) is defined as

$$\text{Fuel-air ratio (unburned)} = \frac{w_{ft} - (w_{f,ph}\eta_{ph}/100)}{w_a - \left(\frac{w_{f,ph}\eta_{ph}/100}{0.067}\right)}$$

where

$w_{ft}$ total fuel-flow rate to both preheater and afterburner, kg/sec (lb/sec)

$w_{f,ph}$ preheater fuel-flow rate, kg/sec (lb/sec)

$\eta_{ph}$ preheater combustion efficiency, percent

$w_a$ total airflow rate, kg/sec (lb/sec)

The terms $f_{ph}$ and $f_{ab}$ are used in the calculation of combustion efficiency. The afterburner fuel-air ratio (unburned) is used only in the discussion and presentation of data.

Combustion efficiency is defined as the ratio of the heat output of the afterburner to the chemical energy of all fuel entering the afterburner. The heat output ($\Delta h_o$, J/kg (Btu/lb)) is equal to

$$\Delta h_o = \Delta h_p + \Delta h_w + q_l$$

where

$\Delta h_p$ change in enthalpy of afterburner propellant fluids (fuel, air, and combustion products), J/kg (Btu/lb)

$\Delta h_w$ change in enthalpy of water used to quench afterburner exhaust gases, J/kg (Btu/lb)

$q_l$ heat losses from system, J/kg (Btu/lb)

In the calculation of $\Delta h_p$, combustion in both the preheater and the afterburner is assumed to occur at a reference temperature of 298 K (537° R), and the products of combustion are assumed to be $CO_2$ and $H_2O$ in the gaseous phase. The enthalpy ($h_m$, J/kg (Btu/lb)) of a leaner-than-stoichiometric burned mixture of fuel and air may be expressed (ref. 8) as

$$h_m = \left[ h_a + f\left(\frac{Am + B}{m + 1}\right) \right]_{T_r}^{T_b}$$

where, for example $\left[h_a\right]_{T_r}^{T_b}$ is used to mean "the value of $h_a$ at $T_b$ minus the value of $h_a$ at $T_r$," and where

$h_a$ enthalpy of air, J/kg (Btu/lb)

f fuel-air ratio

$T_r$ reference temperature equal to 298 K (537° R)

$T_b$ total temperature of burned mixture, K (°R)

m hydrogen-carbon ratio of fuel

$$A = \frac{H_{H_2O} - \frac{1}{2} H_{O_2}}{2.016}$$

$$B = \frac{H_{CO_2} - H_{O_2}}{12.010}$$

and

H molal enthalpy, J/mole (Btu/mole)

The term $(Am + B)/(m + 1)$ accounts for the difference between the enthalpy of the carbon dioxide and water vapor in the burned mixture and the enthalpy of the oxygen removed from the air by their formation.

The expression for $h_m$ may be used to determine the enthalpy of the gases entering the afterburner from the preheater, as well as the enthalpy of the afterburner combustion products. However, prior to expressing $\Delta h_p$ in terms of $h_m$, we should bear in mind that (1) the combustion efficiency of the preheater is explicitly defined in appen-

dix B, (2) the sensible enthalpy of the unburned gasoline entering the afterburner from the preheater is considered negligible, and (3) the enthalpy of the ASTM A-1 fuel is zero since this fuel is assumed to enter the afterburner at the reference temperature. Finally, the change in enthalpy of the afterburner propellant fluids becomes

$$\Delta h_p = \left[ h_a + f_{ph}\left(\frac{As + B}{s + 1}\right) + f_{ab}\left(\frac{Ar + B}{r + 1}\right) \right]_{T_r}^{T_{bal}} - \left[ h_a + f_{ph}\left(\frac{As + B}{s + 1}\right) \right]_{T_r}^{T_{in}}$$

$$= \left[ h_a + f_{ph}\left(\frac{As + B}{s + 1}\right) \right]_{T_{in}}^{T_{bal}} + \left[ f_{ab}\left(\frac{Ar + B}{r + 1}\right) \right]_{T_r}^{T_{bal}}$$

where

| | |
|---|---|
| $f_{ph}$ | fuel-air ratio of preheater |
| $s$ | hydrogen-carbon ratio of preheater fuel |
| $f_{ab}$ | fuel-air ratio of afterburner |
| $r$ | hydrogen-carbon ratio of afterburner fuel |
| $T_{bal}$ | total temperature at enthalpy balance plane, K ($^{o}$R) |
| $T_{in}$ | total temperature at afterburner inlet, K ($^{o}$R) |

The change in enthalpy of the quench water $\Delta h_w$ was computed by assuming that no liquid water is present at the enthalpy balance plane. The expression is as follows

$$\Delta h_w = \left[ \frac{w_q}{w_a} h_w \right]_{T_{w,in}}^{T_{bal}}$$

where

| | |
|---|---|
| $w_q$ | quench-water flow rate, kg/sec (lb/sec) |
| $w_a$ | airflow rate, kg/sec (lb/sec) |
| $h_w$ | enthalpy of water, J/kg (Btu/lb) |
| $T_{w,in}$ | temperature of quench water entering afterburner, K ($^{o}$R) |

The heat losses from the system $q_l$ consist of the energy removed by the two independent water jacket systems and by radiation from the enthalpy balance tube. The heat losses are expressed as

$$q_l = \frac{Q_l}{w_a} = \frac{C}{w_a}(T_{bal})^4 + \sum_{n=1}^{2} \frac{w_{cw,n}}{w_a}(T_{cw,out,n} - T_{cw,in,n})$$

where

| | |
|---|---|
| $Q_l$ | total heat loss, J/sec (Btu/sec) |
| $w_{cw}$ | cooling-water flow rate, kg/sec (lb/sec) |
| $T_{cw,out}$ | cooling-water outlet temperature, K ($^{o}$R) |
| $T_{cw,in}$ | cooling-water inlet temperature, K ($^{o}$R) |
| C | empirical radiation heat-transfer constant, $2.13\times10^{-7}$ J/sec $K^4$ ($1.92\times10^{-11}$ Btu/sec $^{o}R^4$) |

The expression for the total heat output is now

$$\Delta h_o = \left[h_a + f_{ph}\left(\frac{As + B}{s + 1}\right)\right]_{T_{in}}^{T_{bal}} + \left[f_{ab}\left(\frac{Ar + B}{r + 1}\right)\right]_{T_r}^{T_{bal}} + \left[\frac{w_q}{w_a}h_w\right]_{T_{w,in}}^{T_{bal}}$$

$$+ \frac{C}{w_a}(T_{bal})^4 + \sum_{n=1}^{2} \frac{w_{cw,n}}{w_a}(T_{cw,out,n} - T_{cw,in,n})$$

The expression for the chemical energy ($h_c$, J/kg (Btu/lb)) of all fuel entering the afterburner includes the unburned fuel entering the afterburner from the preheater and is written as

$$h_c = \left(1 - \frac{\eta_{ph}}{100}\right) f_{ph} h_{lv,ph} + f_{ab} h_{lv,ab}$$

where

$\eta_{ph}$ combustion efficiency of preheater, percent

$h_{lv,ph}$ lower heating value of preheater fuel at $T_r$, J/kg (Btu/lb)

$h_{lv,ab}$ lower heating value of afterburner fuel at $T_r$, J/kg (Btu/lb)

Now, the combustion efficiency, obtained by dividing the heat output of the afterburner $\Delta h_o$ by the chemical energy of the available fuel $h_c$, is

$$\text{Combustion efficiency} = \left\{ \frac{\left[h_a + f_{ph}\left(\frac{As+B}{s+1}\right)\right]_{T_{in}}^{T_{bal}} + \left[f_{ab}\left(\frac{Ar+B}{r+1}\right)\right]_{T_r}^{T_{bal}}}{\left(1 - \frac{\eta_{ph}}{100}\right) f_{ph} h_{lv,ph} + f_{ab} h_{lv,ab}} \right.$$

$$\left. + \frac{\frac{w_q}{w_a} h_w \Big|_{T_{w,in}}^{T_{bal}} + \frac{C}{w_a}(T_{bal})^4 + \sum_{n=1}^{2} \frac{w_{cw,n}}{w_a}(T_{cw,out,n} - T_{cw,in,n})}{1 - \frac{\eta_{ph}}{100} f_{ph} h_{lv,ph} + f_{ab} h_{lv,ab}} \right\} \times 100$$

The thermodynamic values used in the calculation of combustion efficiency are

| | |
|---|---|
| Hydrogen-carbon ratio of the afterburner fuel, r | 0.161 |
| Hydrogen-carbon ratio of the preheater fuel, s | 0.178 |
| Lower heating value of preheater fuel at $T_r$, $h_{lv,ph}$, J/kg (Btu/lb) | 43 920 (18 900) |
| Lower heating value of afterburner fuel at $T_r$, $h_{lv,ab}$, J/kg (Btu/lb) | 43 230 (18 600) |

# APPENDIX B

# OPERATING CHARACTRRISTICS OF TEST APPARATUS

## General

The gases should be carefully conditioned at the inlet and again at the outlet of the afterburner combustion chamber. The behavior of the components that did this conditioning was examined and is described herein. Also, time response of the test apparatus is discussed.

## Quality of Afterburner Inlet Flow

Three important properties of the gas flow field entering the afterburner are (1) the combustion efficiency of the vitiating preheater, (2) the gas temperature profile, and (3) the gas velocity profile.

The preheater combustion efficiency was measured by several means. The 40 thermocouples (fig. 9) located as shown in figure 2 provided the basic measuring technique; however, on several occasions, an analysis of the composition of the preheater exhaust gases was used to substantiate the thermocouple-determined efficiency. The combustion efficiency data were fit by the equation

$$100 - \frac{15 - 803f + 15\,120f^2}{1.86\left(\frac{T}{560}\right)^2 - 0.86\left(\frac{T}{560}\right)}$$

where

f fuel-air ratio

T inlet-air temperature, $^{o}R$

The equation, applicable for flow conditions that correspond to afterburner-inlet pressure of 1 atmosphere and velocity of 150 meters per second (500 ft/sec), respectively, is plotted in figure 17. The preheater combustion efficiency used in the calculations was taken to be 97 percent at test condition A, 97.8 percent at test condition B, and 98.4 percent at test condition C.

The fuel nozzles were unmodified. Each can contained a cluster of six nozzle units,

as shown in figure 3. In turn, each nozzle unit contained two concentric nozzles: an inner primary (fine spray) and an outer secondary (coarse spray). Fuel nozzle manifolding permitted separate flow control for the two sets of sprays. When the nozzle pressure was sufficient to permit the formation of a cone spray, the combustion efficiency was unaffected by the flow split between primary and secondary nozzles. At the 450 K (350° F) preheater inlet-air temperature, the nozzles remained clean and hence the temperature profile data typified by figure 18 remained invariant throughout the project.

Inlet Mach number profiles obtained at the fuel injector plane (fig. 5) for test condition A are presented in figure 19. The lobed profile (fig. 19(b)) was obtained without baffles, and the flat profile (fig. 19(a)) was obtained with the baffle shown in figure 5. The velocity data were obtained with a pitot-static array located at the sites shown in figure 19. Since the profile is dependent on the nature of the flameholder blockage, a dummy flameholder consisting of a set of parallel V-gutters was located 12.7 centimeters (5 in.) downstream of the pressure sensing array.

## Quench of Afterburner Exhaust Flow

The flame quench and enthalpy balance system are closely related. The quench system must stop the flame at a well-defined plane normal to the flow. Otherwise, combustor length would be vague and combustion efficiency values meaningless. At the exit of the calorimeter, all water from the quench and combustion products must be vaporized in order that the proper value of fluid enthalpy can be assigned. Nor can the enthalpy of the exiting fluid be defined accurately unless the temperature is properly measured.

Flame quenching provided by the spray head (fig. 6) was judged to be satisfactory. The vanes (fig. 2) provided the mixing required to vaporize all the water. However, experience showed complete vaporization was not assured unless the average exit temperature was in excess of 700 K (800° F). The error in combustion efficiency resulting from too much water (too small a value of exhaust temperature) can be illustrated with the aid of figure 20. The data shown are for a fixed value of the afterburner operating conditions. Only the quench-water flow rate was varied. An increase in water flow rate that decreased the average temperature from 855 to 655 K (1080° to 720° F) caused no change in the computed value of combustion efficiency, 96.5 percent; however, a further decrease of like amount resulted in an efficiency decrease of 11 percentage units. The source of the observed error is the presence of liquid water. When the local stream temperature is a trifle too cool, small amounts of water do not have time to evaporate. The liquid impinges on the associated thermocouple and chills it. Chilling is shown in figure 21. Each of the three bar charts presents the individual thermocouple values that were arithmetically averaged to obtain the calorimeter exit-plane temperature. The

three data sets correspond to the three marked data points forming the knee of the data curve of figure 20. For data set 3646, no liquid water is present; however, for data set 3647, sufficient liquid exists to drastically chill one thermocouple (as shown in fig. 21(b)) and to force downward the computed value of combustion efficiency. The next data set (3648) represents a further addition of quench water. Three couples are shown in figure 21(c) to be severely chilled and the computed value of efficiency undergoes a further decline.

On the other hand, whenever the gases at the calorimeter exit plane become too hot, either locally or as an average, the casing walls would tend to warp. A number of studies indicated that neither hardware damage nor combustion efficiency error due to liquid water would occur provided (1) the average gas temperature at the calorimeter exit was kept within bounds of 700 to 870 K ($800^{\circ}$ to $1100^{\circ}$ F); (2) the minimum permissible, individual thermocouple temperature was in excess of 610 K ($640^{\circ}$ F); and (3) the pipe temperature of the enthalpy balance casing at the exit plane was maintained at temperatures above 560 K ($550^{\circ}$ F). In order to attain the necessary control of the gas temperature profile, the three sets of quench-water sprays described in the section APPARATUS were utilized to the utmost.

The other important reason for striving towards a uniform temperature profile was to obtain reliable values of average gas temperature for use in the calculations. Ideally, a warped profile should be mass-weighted in order to obtain the proper temperature value. However, gas exit temperature was measured as an arithmetic average of the individual thermocouple readings. The resulting effect on combustion efficiency values was examined. A typical spread of individual thermocouple values is shown in figure 21(a). A shift in profile (obtained by rerouting the quench water from one set of sprays to another) showed little or no effect on the combustion efficiency value, provided the temperature restraints of the preceding discussion were adhered to. Further evidence that the temperature-averaging technique was satisfactory is demonstrated in figure 20. Therein, and in all other cases examined, a plateau exists where combustion efficiency is invariant for a range of gas temperatures, although the spread of the temperature profile changes with a change in average temperature.

## Time Response

Because of thermal lag, the calorimeter technique of obtaining combustion efficiency data is assumed to be a time-consuming process. However, the present apparatus permitted data to be taken in a relatively rapid manner. The time interval between data sets was approximately 3 minutes for data being taken as described in the section PROCEDURE. Namely, once a given afterburner inlet condition had been established,

the test crew manipulated only the afterburner fuel, water-quench, and combustor-pressure valves when changing from one set point to another.

Figures 22 and 23 illustrate the time response of the apparatus to step changes in the control settings. Figure 22 shows the response for a modest step change in quench-water flow rate (fuel flow rate held constant). Approximately 6 minutes were required for the apparatus to establish a new equilibrium value of pipe temperature. However, the computed value of combustion efficiency is shown to restore itself within a period of 2 minutes. Figure 23 illustrates step changes that were made in fuel-air ratio (fuel flow rate) at all three inlet temperatures. For these experiments, the quench-water flow rates were adjusted in order to keep calorimeter-exit and pipe-exit temperatures unchanged from selected preset values. Although the fuel-air ratio changes produced significant changes in the values of combustion efficiency, the new efficiency values were arrived at so rapidly that a transition curve could not be faired through the data.

# APPENDIX C

# COMBUSTION EFFICIENCY ERROR

## Probable Error

In order to estimate the accuracy of combustion efficiency values obtained by the calorimeter technique, a numerical study of probable combustion efficiency error was undertaken. The approach used was to start with a set of actual performance program input data. The data set was submitted repeatedly as input to the performance analysis program. With each input, however, one of the parameters affecting combustion efficiency was assigned a 1-percent increase from its original value. All other parameters were left unaltered. From the computed results the error in combustion efficiency due to a 1-percent error in the parameter could be obtained. The aforementioned approach was applied to three sets of performance program input data and the results are presented in table I. The three data sets are for a fuel-air ratio of 0.03 at an inlet temperature of 920 K (1200° F) and for fuel-air ratios of 0.015 and 0.03 at an inlet temperature of 1255 K (1800° F). For each data set, table I lists the unaltered value of the parameter, immediately followed by the value of the error in combustion efficiency.

To arrive at a probable efficiency error due to the combined effect of all parameters, a statistical error formula was used:

$$\Delta\eta = \left[\sum_{i=1}^{N} \left(\frac{\Delta\eta_i}{\Delta X_i}\right)^2 \times (\Delta X_i)^2\right]^{1/2}$$

where

| | |
|---|---|
| $\Delta\eta$ | probable error ($3\sigma$ variation of combustion efficiency $\eta$) |
| $\Delta\eta_i/\Delta X_i$ | error in combustion efficiency $\eta$ caused by a 1-percent error in parameter $X_i$ (see table I) |
| $\Delta X_i$ | $3\sigma$ variation of parameter $X_i$ (see table I) |
| N | number of parameters (7) |

The quantity $\Delta X_i$ is the authors' estimate of the probable error of each parameter. The value $\Delta X_i$ is shown in the right-most column of table I and is assumed to apply equally to all three data sets. Finally, the probable error in combustion efficiency for the three sets of data are as follows:

| Data set | Combustion efficiency, $\Delta\eta$, percent |
|---|---|
| Inlet temperature, 920 K (1200° F); fuel air ratio, 0.030 | 3.1 |
| Inlet temperature, 1255 K (1800° F); fuel air ratio, 0.030 | 4.2 |
| Inlet temperature, 1255 K (1800° F); fuel-air ratio, 0.015 | 6.8 |

These results provide a warning that combustion efficiency comparisons discussed in the body of the report should not be of hair-splitting detail. Also, the table I data show those factors that promote significant error and where the larger values of error would be expected to occur in the test results of figures 10, 11, and 15.

## Dissociation Effects

The combustion efficiency values as computed are very likely too small under certain circumstances. The equation assumes the combustion products leaving the calorimeter were carbon dioxide and water vapor. However, at near-stoichiometric fuel-air ratios some of the gases entering the water-quench plane were dissociated. The water spray cooled the gases rapidly, probably freezing the composition at the high-temperature equilibrium level (ref. 9). The dissociation enthalpy, therefore, was not recovered as measurable sensible enthalpy as the products cooled. Conceivably, this unrecovered enthalpy could have penalized the combustion efficiency data by 10 percent in the most severe instance - afterburner at stoichiometric mixture and preheater at 1255 K (1800° F). The foregoing argument is supported by the calculation of carbon monoxide oxidation rates discussed in reference 10.

# REFERENCES


1. Reck, Gregory M.; Branstetter, J. Robert; and Diehl, Larry A.: Preliminary Sector Tests at 920 K (1200° F) of Three Afterburner Concepts Applicable for Higher Inlet Temperatures. NASA TN D-6437, 1971.

2. Curry, John J.: Requirements for Advancement of Technology, Thrust Augmentation Systems. Rep. NAPTC-ATD-173, Naval Air Propulsion Test Center, 1969.

3. King, Charles R.: A Semiempirical Correlation of Afterburner Combustion Efficiency and Lean-Blowout Fuel-Air-Ratio Data with Several Afterburner-Inlet Variables and Afterburner Lengths. NACA RM E57F26, 1957.

4. Mealey, Charles; and Kee, Leslie: A Computer-Controlled Central Digital Data Acquisition System. NASA TN D-3904, 1967.

5. Staff of the Lewis Laboratory: Central Automatic Data Processing System. NACA TN 4212, 1958.

6. Olson, Walter T.: Combustion Chamber Development. Design and Performance of Gas Turbine Power Plants. Vol. XI of High Speed Aerodynamics and Jet Propulsion. W. R. Hawthorne and W. T. Olson, eds., Princeton Univ. Press, 1960, pp. 289-350.

7. Childs, J. Howard: Flame Stabilization. Design and Performance of Gas Turbine Power Plants. Vol. XI of High Speed Aerodynamics and Jet Propulsion. W. R. Hawthorne and W. T. Olson, eds., Princeton Univ. Press, 1960, pp. 119-165.

8. Turner, L. Richard; and Lord, Albert M.: Thermodynamic Charts for the Computation of Combustion and Mixture Temperatures at Constant Pressure. NACA TN 1086, 1946.

9. Reynolds, Thaine W.; and Haas, Donald P.: Performance of Slurries of 50 Percent Boron in JP-4 Fuel in 5-Inch Ram-Jet Burner. NACA RM E54D07, 1954.

10. Brokaw, Richard S.; and Bittker, David A.: Carbon Monoxide Removal Under Automotive Thermal Reactor Conditions. Inst. Control Sys., vol. 44, no. 10, Oct. 1971, pp. 103-105.

TABLE I. - SUMMARY OF COMBUSTION EFFICIENCY ERROR

| Parameter | Inlet temperature,[a] K (°R) | | | | | | 3σ variation of parameter $X_i^c$, $\Delta X_i$, percent |
|---|---|---|---|---|---|---|---|
| | 920(1660) | | 1255(2260) | | 1255(2260) | | |
| | Velocity,[a] m/sec (ft/sec) | | | | | | |
| | 150(500) | | 150(500) | | 150(500) | | |
| | Fuel-air ratio (unburned)[a] | | | | | | |
| | 0.03 | | 0.03 | | 0.015 | | |
| | Parameter value | Error in combustion efficiency[b] | Parameter value | Error in combustion efficiency[b] | Parameter value | Error in combustion efficiency[b] | |
| Airflow rate, $w_a$, kg/sec (lb/sec) | 11.44 (25.24) | +0.36 | 8.06 (17.74) | +0.30 | 8.06 (17.74) | +0.59 | 1 |
| Preheater fuel flow rate, $w_{f,ph}$, kg/sec (lb/sec) | 0.1395 (0.3078) | -0.56 | 0.1763 (0.3889) | -1.03 | 0.1761 (0.3882) | -1.98 | 1 |
| Afterburner fuel flow rate, $w_{f,ab}$, kg/sec (lb/sec) | 0.2868 (0.6324) | -0.86 | 0.1618 (0.3567) | -0.98 | 0.0828 (0.1823) | -0.94 | 1 |
| Heat losses, $Q_l$, J/sec (Btu/sec) | 503 000 (475.6) | +0.05 | 605 000 (572.7) | +0.09 | 556 000 (526.3) | +0.15 | 5 |
| Total temperature of gases at enthalpy balance plane, $T_{bal}$, K (°R) | 739 (1329.7) | +1.30 | 725 (1306.3) | +1.77 | 730 (1310.8) | +2.95 | 2 |
| Total temperature of air at inlet of preheater, $T_a$, K (°R) | 453 (815.7) | -0.52 | 454 (816.7) | -0.45 | 455 (818.0) | -0.86 | 1 |
| Quench-water flow rate, $w_q$, kg/sec (lb/sec) | 3.938 (8.687) | +1.03 | 3.550 (7.830) | +1.65 | 2.504 (5.516) | +2.22 | 1 |
| Unperturbed combustion efficiency, percent | 91.0 | | 103.7 | | 101.6 | | |
| Probable error, percent | 3.1 | | 4.2 | | 6.8 | | |

[a]Nominal values.

[b]Measured as increase in value of combustion efficiency resulting from a 1-percent increase in value of listed parameter.

[c]Authors' estimate.

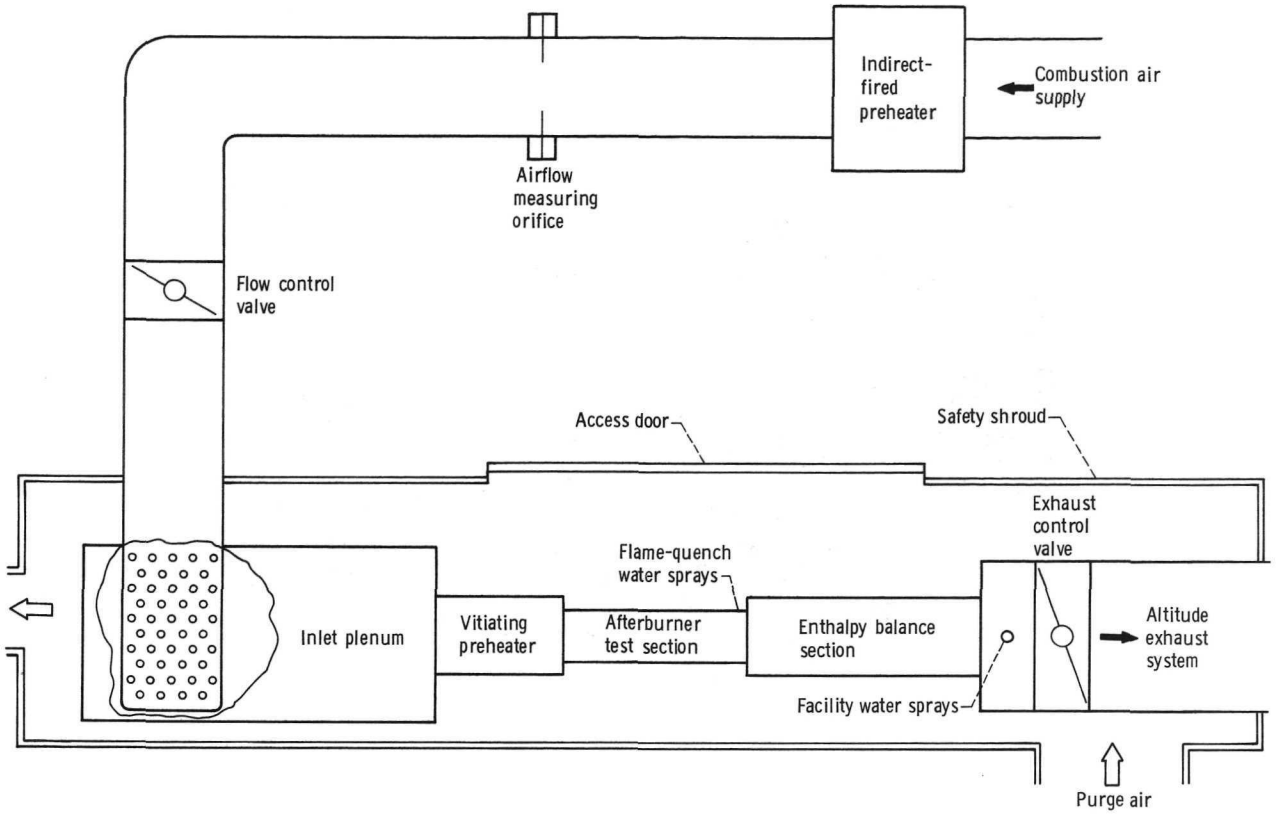


Figure 1. - Schematic diagram of afterburner test facility.

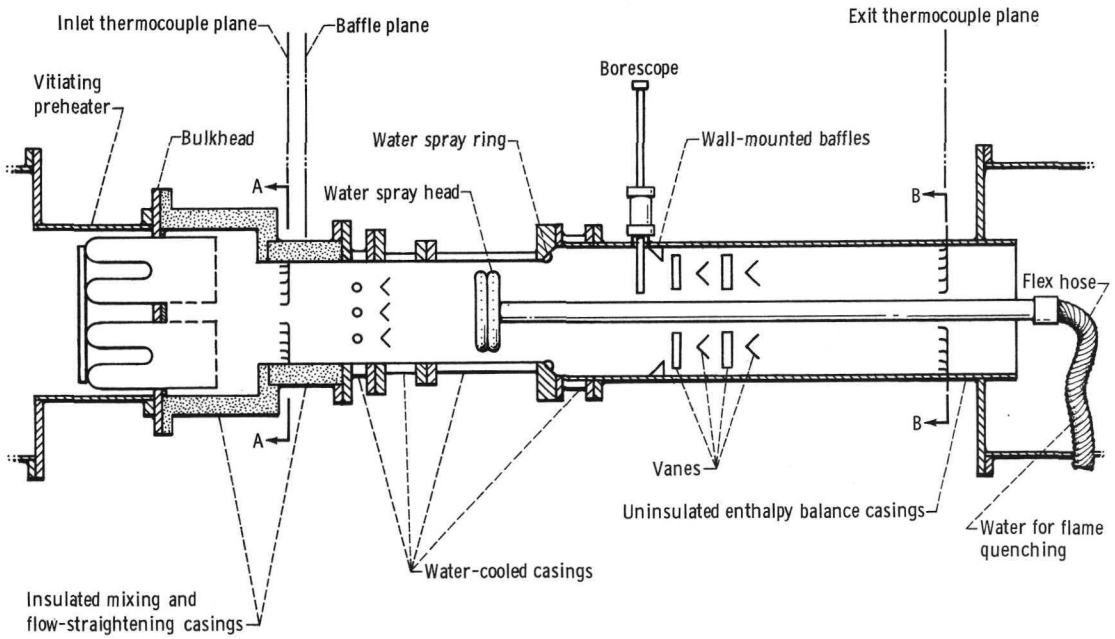


Figure 2. - Diagram of test apparatus.

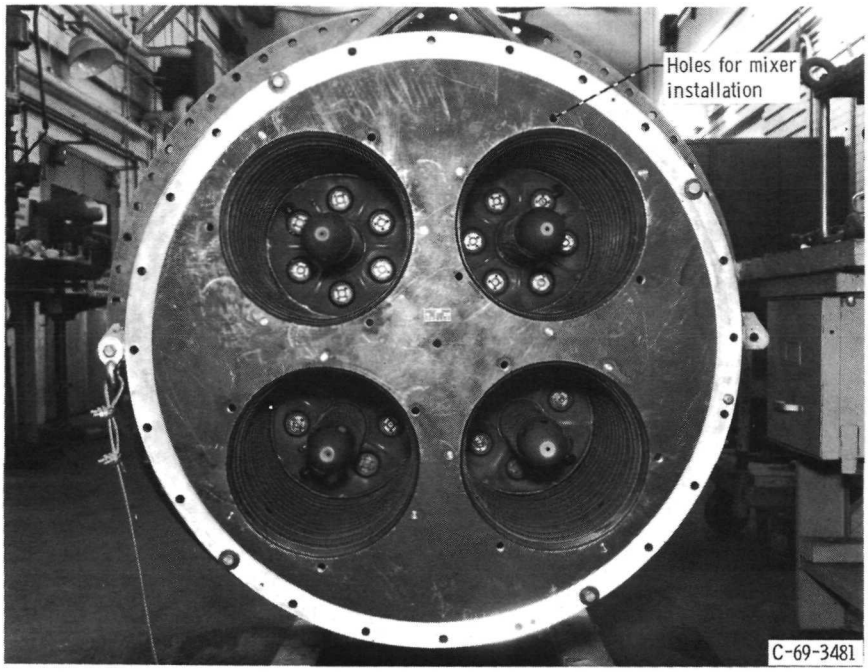


Figure 3. - Combustor cans of vitiating preheater.

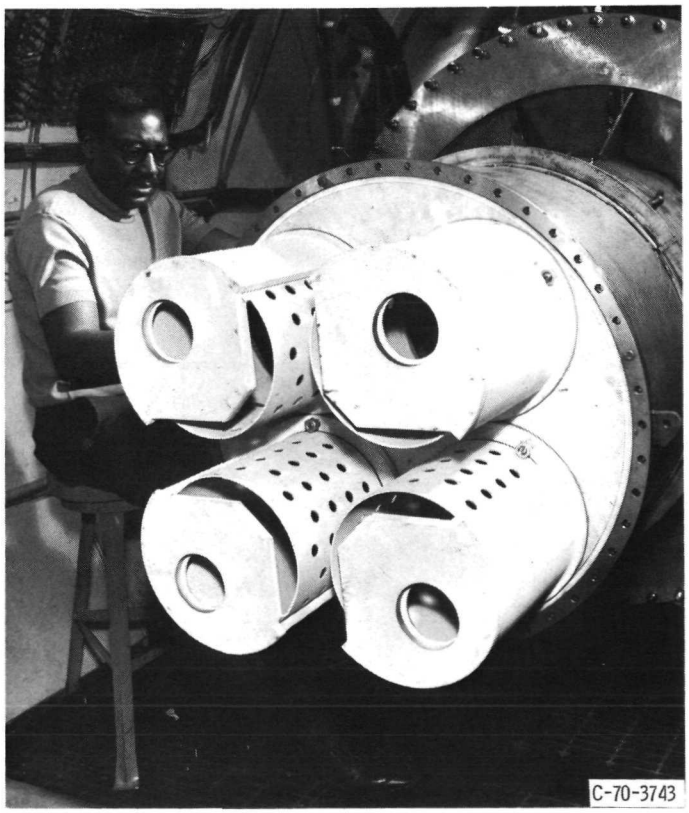


Figure 4. - Mixers mounted on bulkhead.

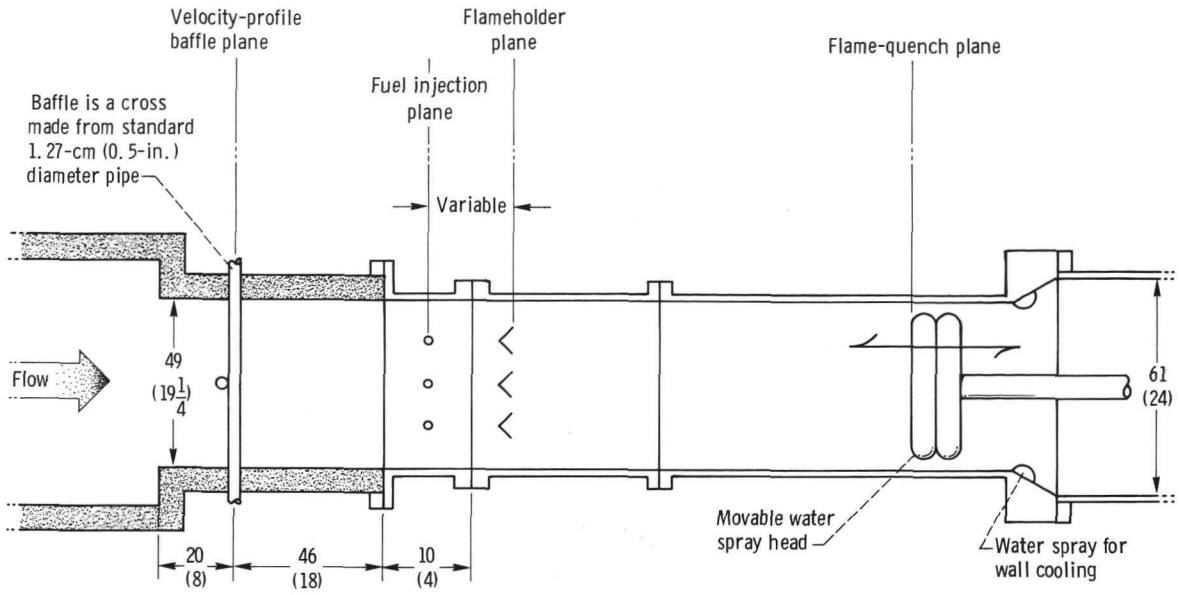


Figure 5. - Cross-sectional view of afterburner test section. Dimensions are in centimeters (in.).

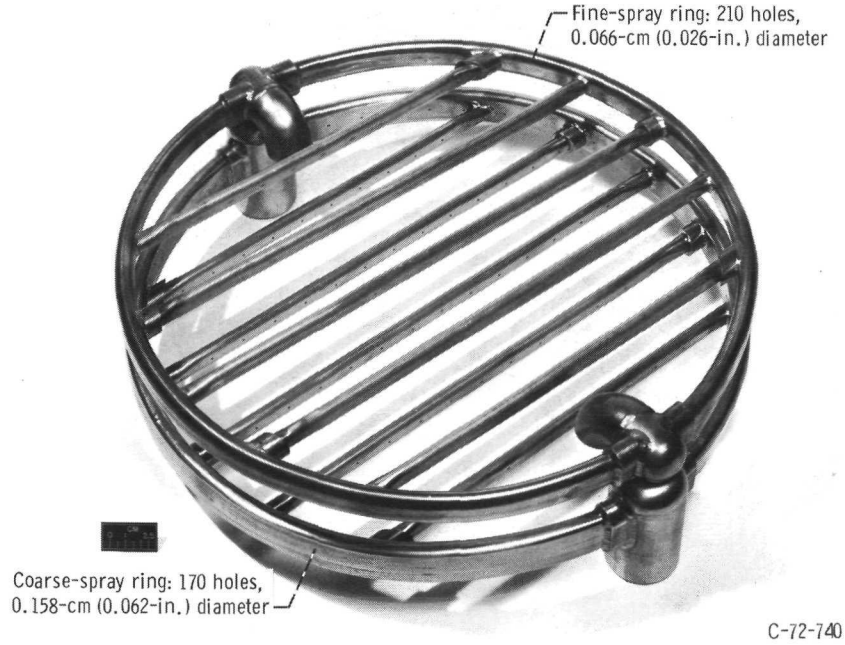


Figure 6. - Flame-quenching water spray head viewed looking downstream.

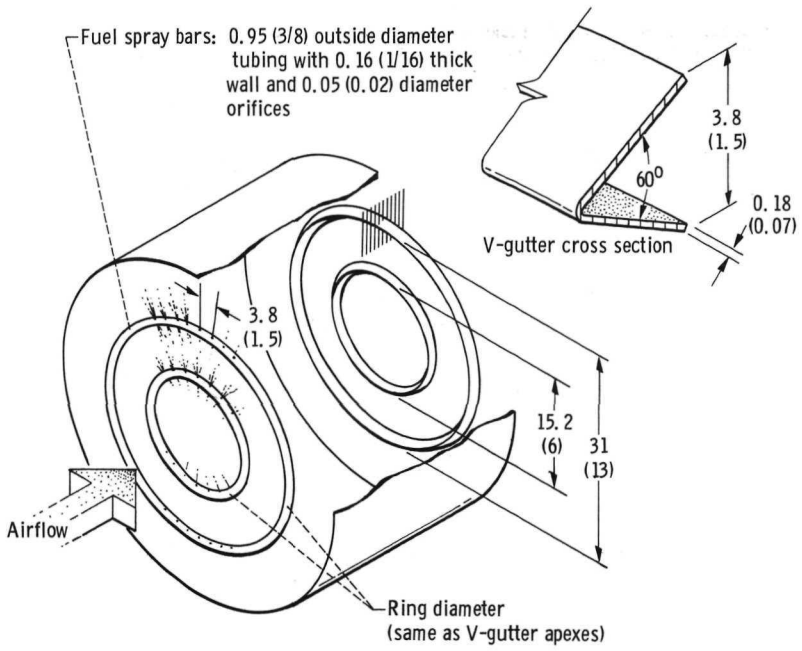


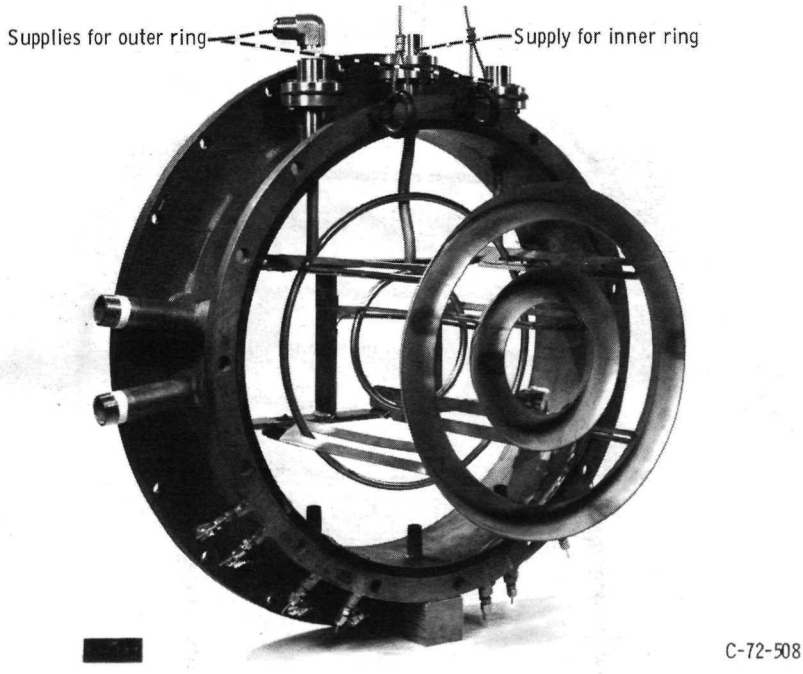


Figure 7. - Circular V-gutter assembly. Dimensions are in centimeters (in.).

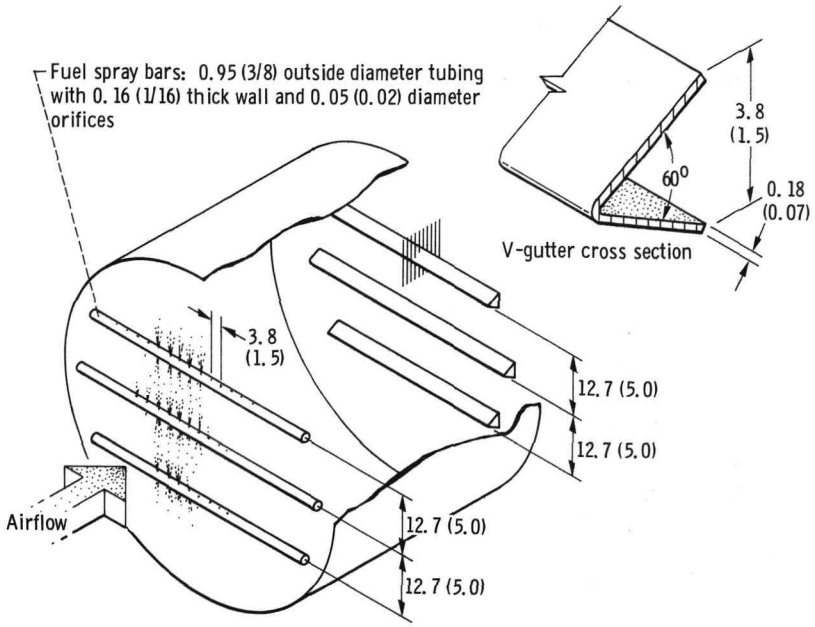


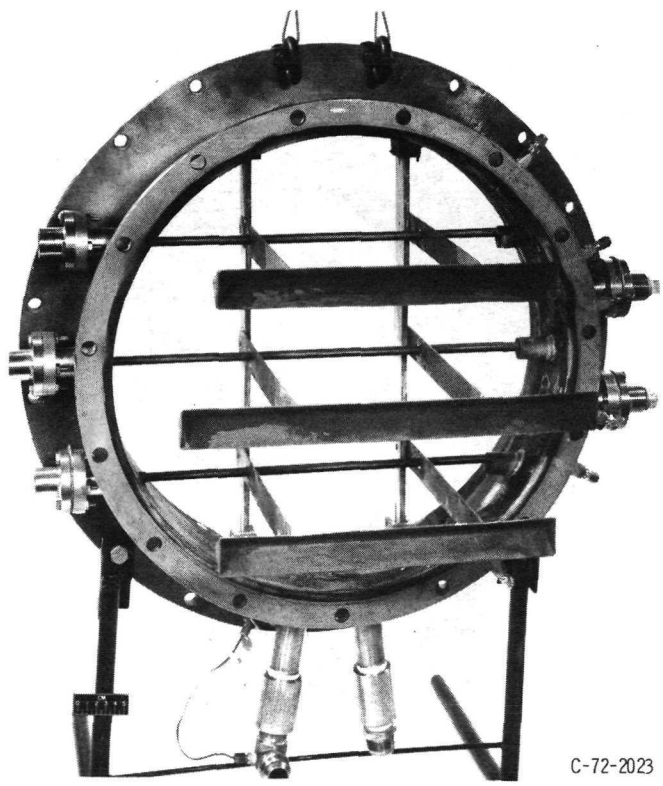


Figure 8. - Parallel V-gutter assembly.

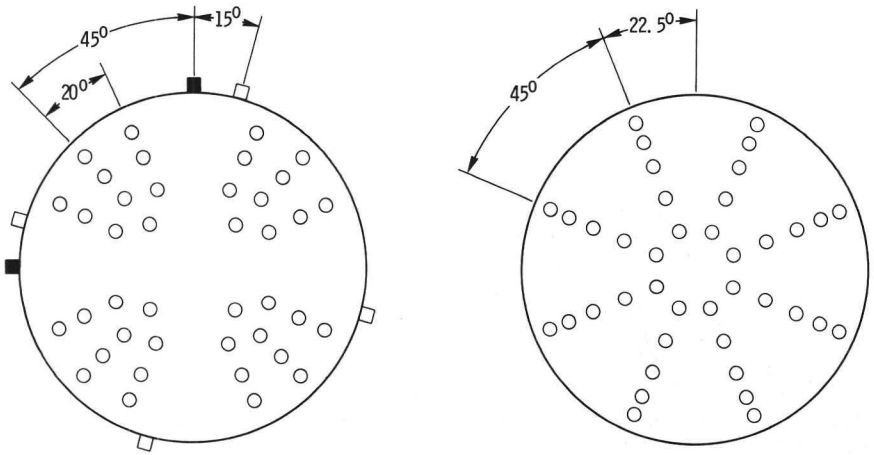


Section A-A
(inlet thermocouple plane of fig. 2)

Section B-B
(exit thermocouple plane of fig. 2)

○ Total temperature thermcouple
□ Static pressure tap
■ Dynamic pressure sensor

Figure 9. - Afterburner instrumentation.

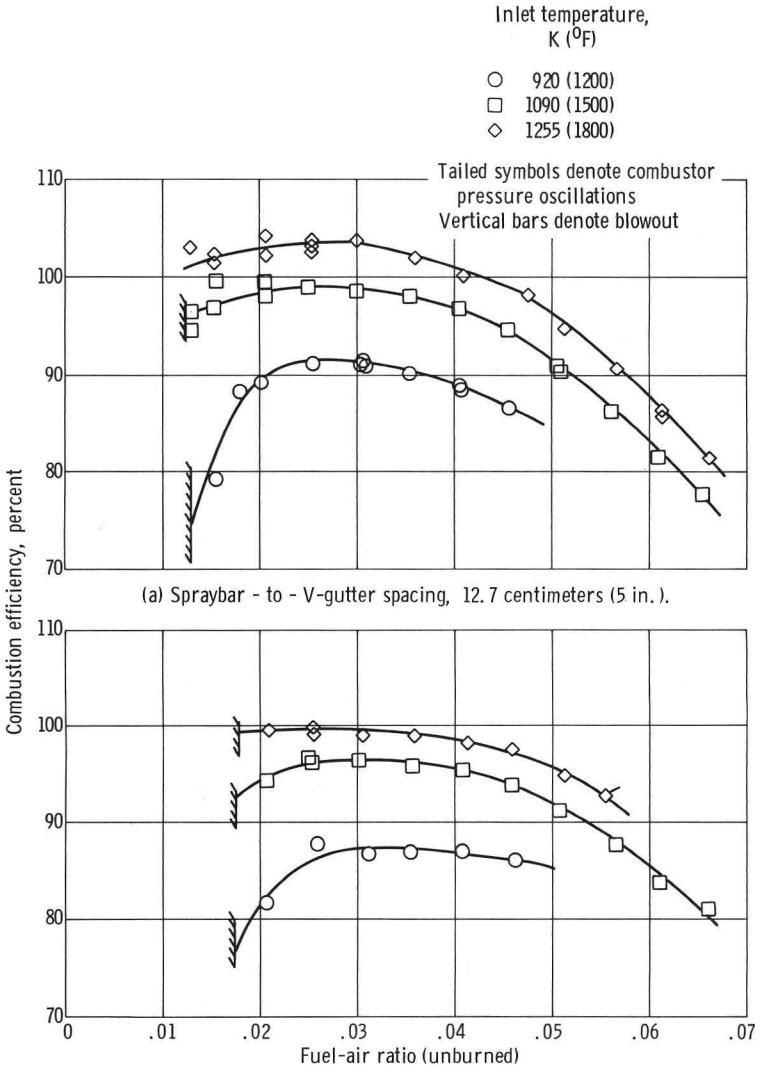


(a) Spraybar - to - V-gutter spacing, 12.7 centimeters (5 in.).

(b) Spraybar - to - V-gutter spacing, 25.4 centimeters (10 in.).

Figure 10. - Combustion performance of circular V-gutters. Lobed velocity profile; average velocity, 150 meters per second (500 ft/sec); inlet static pressure, 1 atmosphere.

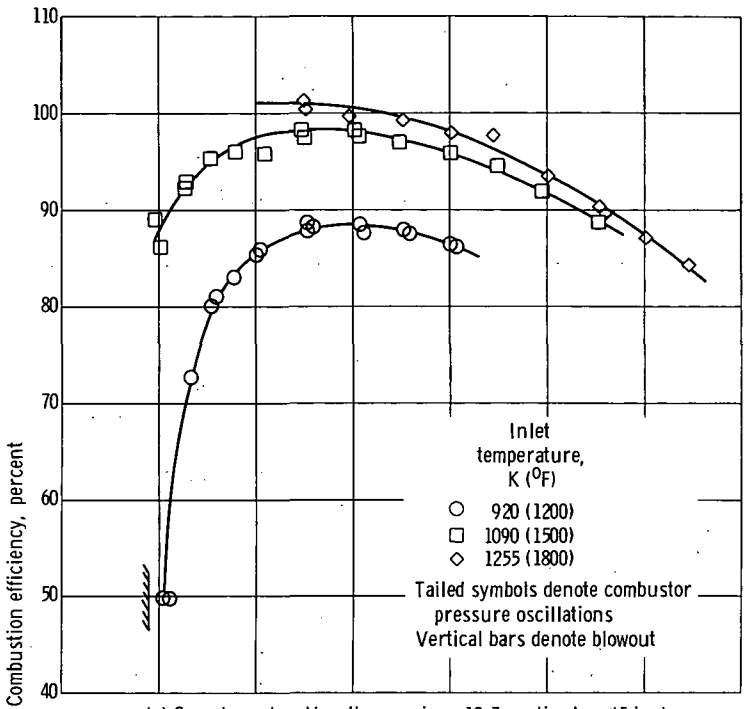


(a) Spraybar - to - V-gutter spacing, 12.7 centimeters (5 in.).

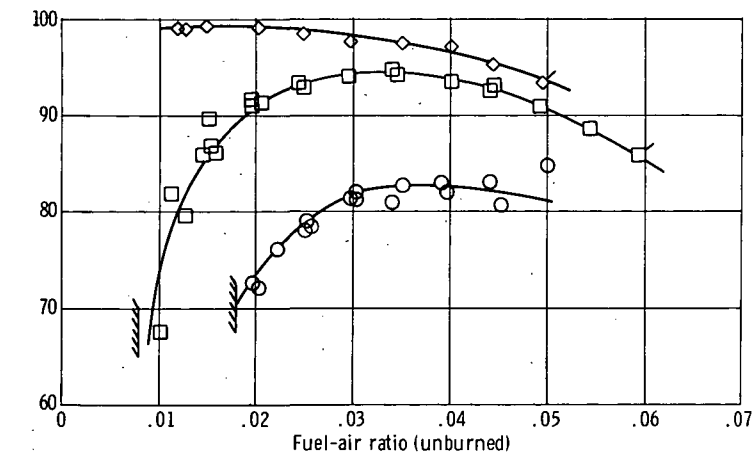


(b) Spraybar - to - V-gutter spacing, 25.4 centimeters (10 in.).

Figure 11. - Combustion performance of parallel V-gutters. Lobed velocity profile; average velocity, 150 meters per second (500 ft/sec); inlet static pressure, 1 atmosphere.

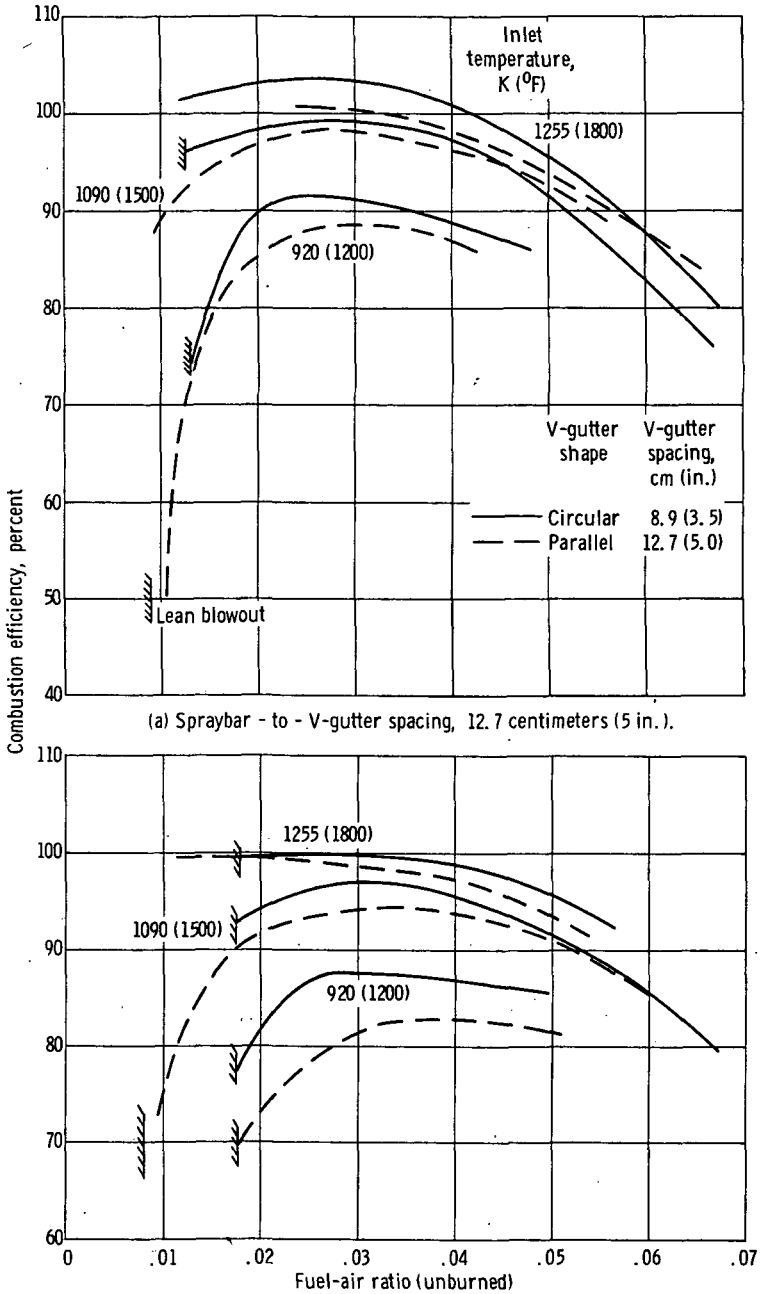


(a) Spraybar - to - V-gutter spacing, 12.7 centimeters (5 in.).

(b) Spraybar - to - V-gutter spacing, 25.4 centimeters (10 in.).

Figure 12. - Combustion efficiency comparison of parallel and circular V-gutters. Data curves are from figures 10 and 11.

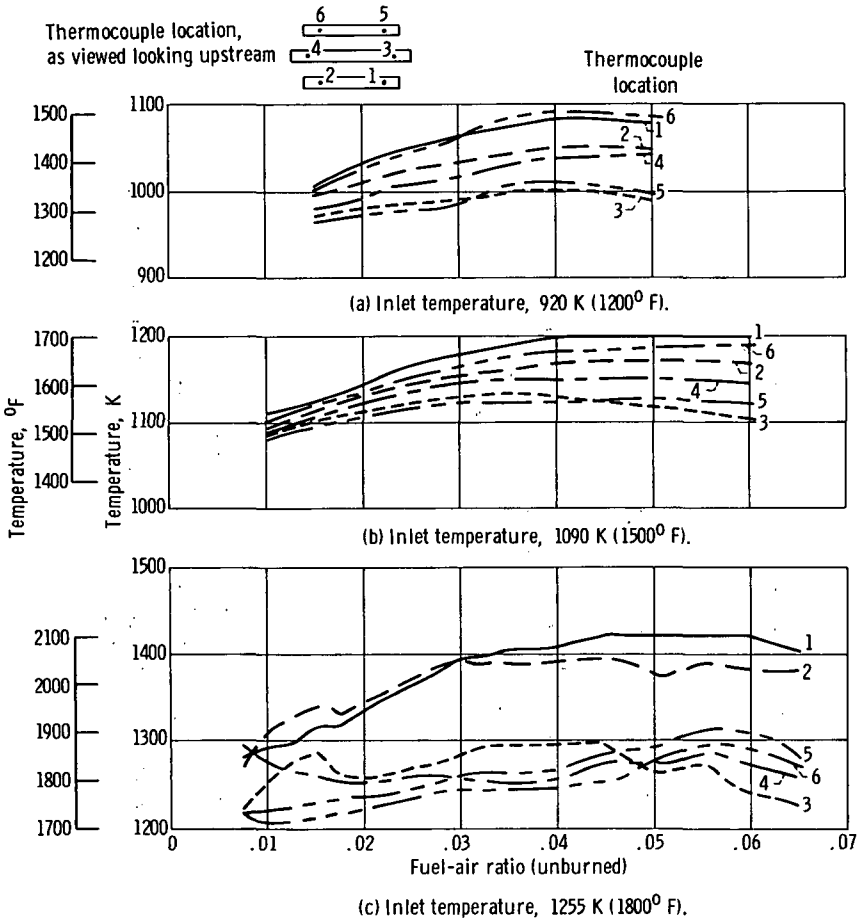


Figure 13. - Metal temperatures of parallel V-gutters as measured by individual thermocouples. Spraybar - to - V-gutter spacing, 25.4 centimeters (10 in.); inlet velocity, 150 meters per second (500 ft/sec); inlet static pressure, 1 atmosphere; lobed velocity profile.

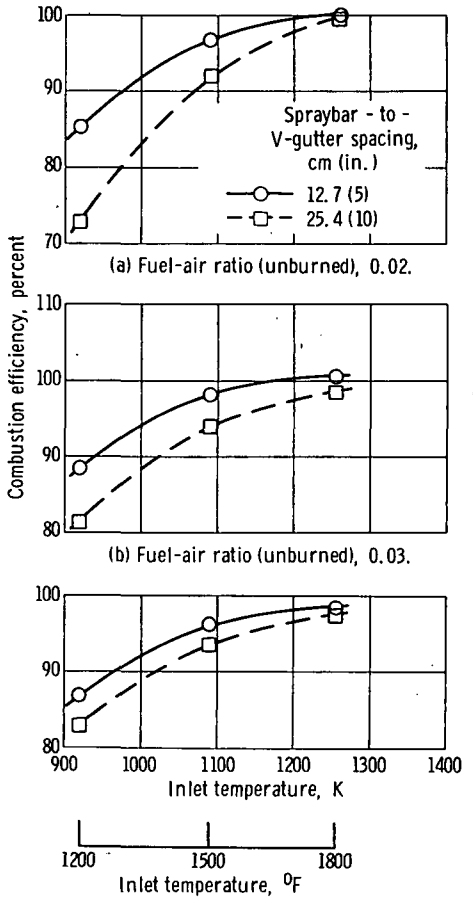


Figure 14. - Effect of inlet temperature and fuel mixing distance on combustion efficiency. Parallel geometry.

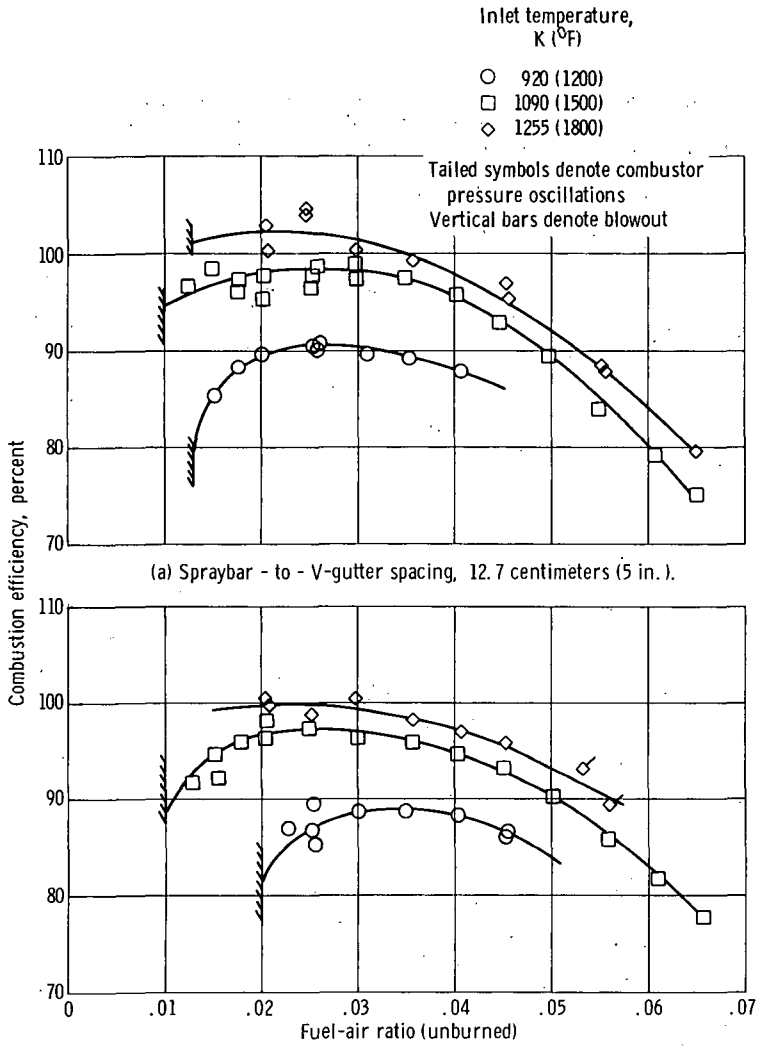


(a) Spraybar - to - V-gutter spacing, 12.7 centimeters (5 in.).

(b) Spraybar - to - V-gutter spacing, 12.7 centimeters (10 in.).

Figure 15. - Combustion performance of circular V-gutters for flat velocity profile. Average velocity, 150 meters per second (500 ft/sec); inlet static pressure, 1 atmosphere.

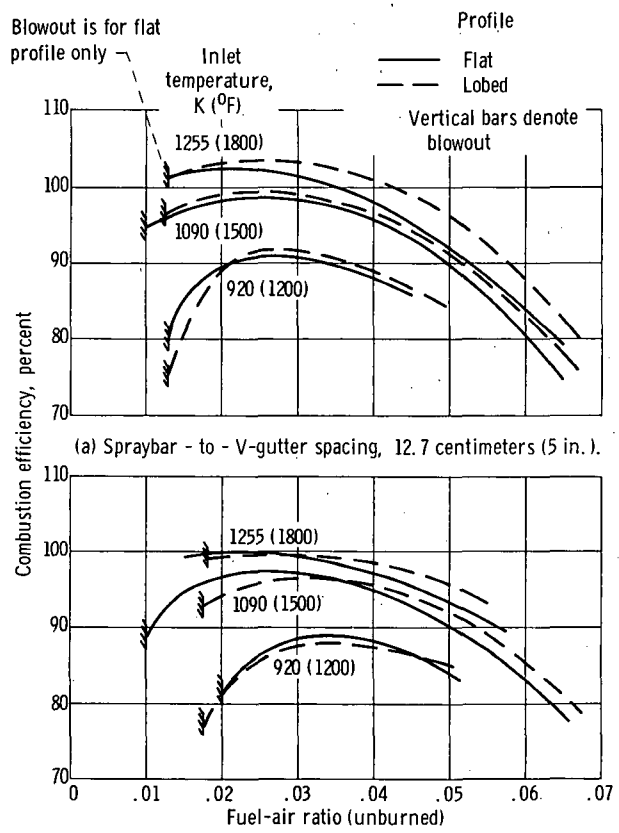


(a) Spraybar - to - V-gutter spacing, 12.7 centimeters (5 in.).

(b) Spraybar - to - V-gutter spacing, 25.4 centimeters (10 in.).

Figure 16. - Influence of inlet-velocity profile on combustion performance. Circular V-gutters.

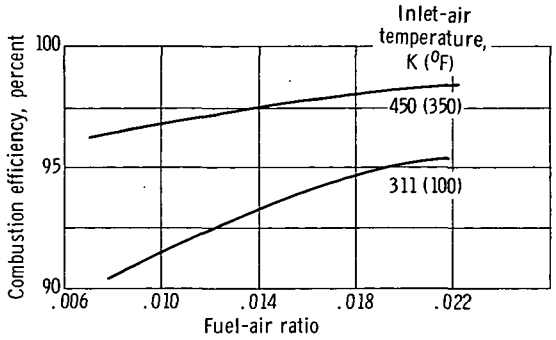


Figure 17. - Combustion efficiency of vitiated preheater. Fuel, clear gasoline. Conditions correspond to afterburner-inlet static pressure and velocity of 1 atmosphere and 150 meters per second (500 ft/sec), respectively.

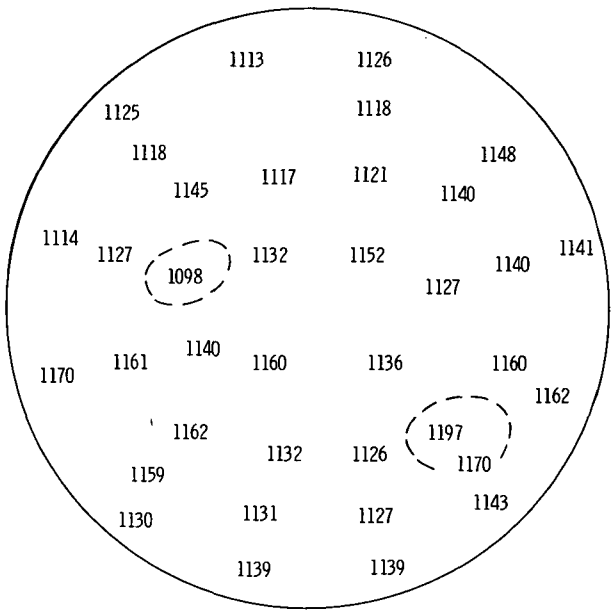


Figure 18. - Temperature pattern (in kelvin) obtained at afterburner inlet thermocouple plane of figure 2. Afterburner inlet velocity, 150 meters per second (500 ft/sec); afterburner inlet static pressure, 1 atmosphere; preheater inlet temperature, 450 K (350° F); preheater fuel-air ratio, 0.0187. Dashed circles enclose temperature values that deviate by more than 30 kelvin from the average temperature, 1140 K (1592° F).

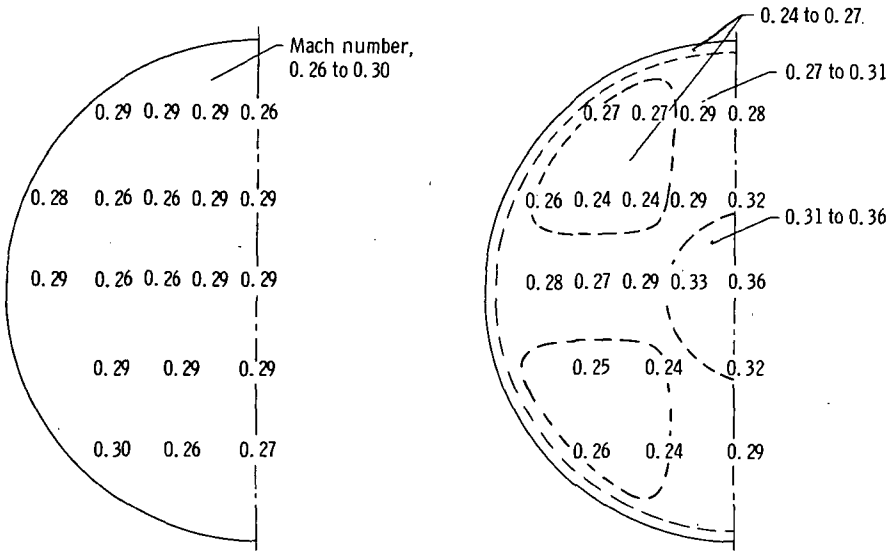


(a) Flat profile. Baffle in place.

(b) Lobed profile. No baffle.

Figure 19. - Mach number profiles obtained at fuel-injector plane of flameholder casing. Test condition A; average Mach number computed from gas flow rate, 0.275.

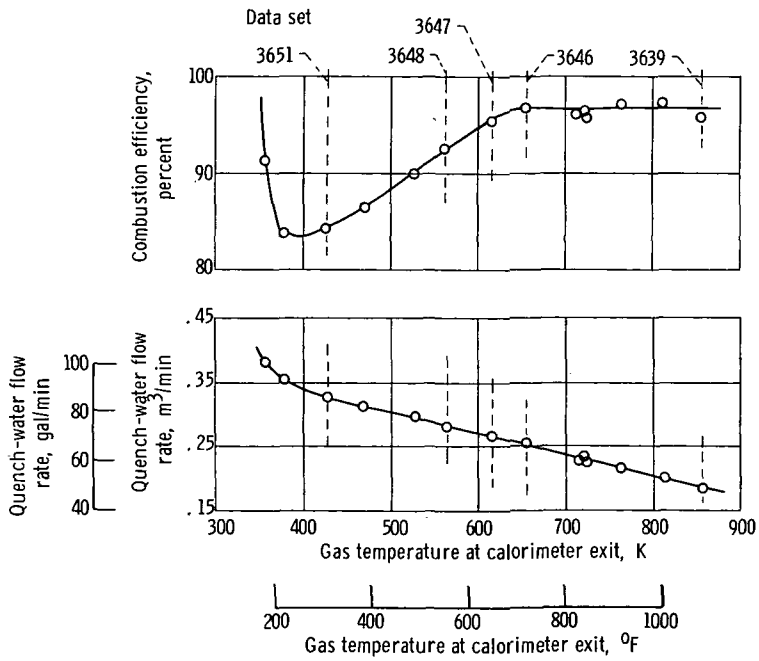


Figure 20. - Effect of gas temperature at calorimeter exit plane on computed value of combustion efficiency. Parallel V-gutters; test condition B; afterburner fuel-air ratio (unburned), 0.03.

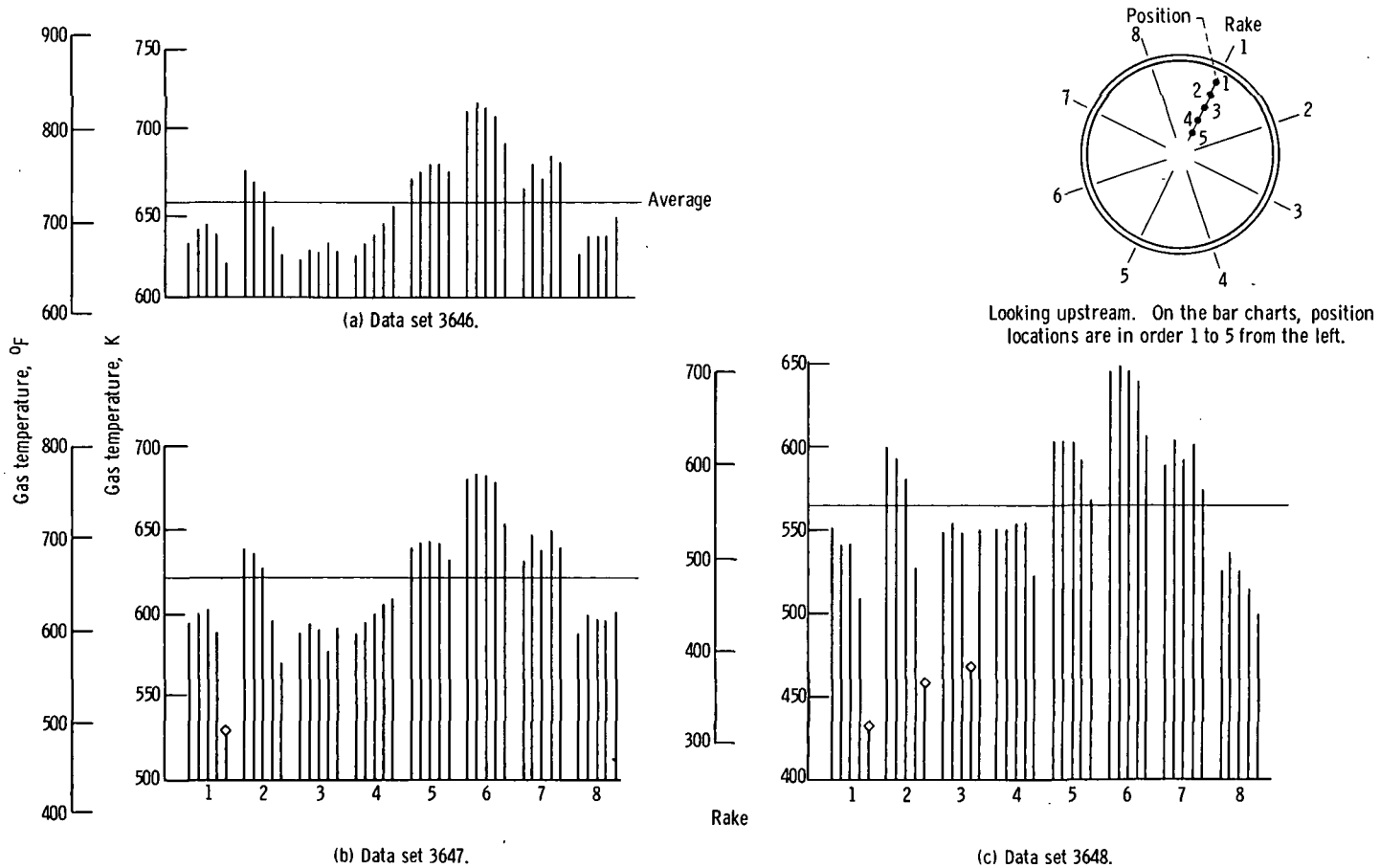


Figure 21. - Gas temperature profiles at calorimeter exit for selected data sets shown in figure 20. Severely chilled thermocouples are marked with symbol ◇ .

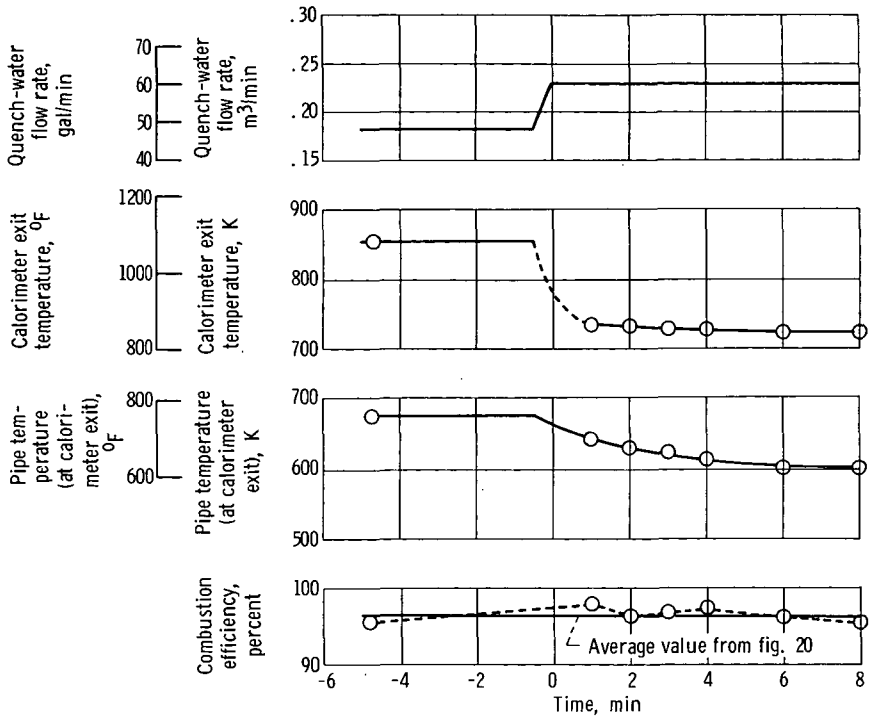


Figure 22. - Response of apparatus to a step change in quench-water flow rate. Test condition B; afterburner fuel-air ratio (unburned), 0.03.

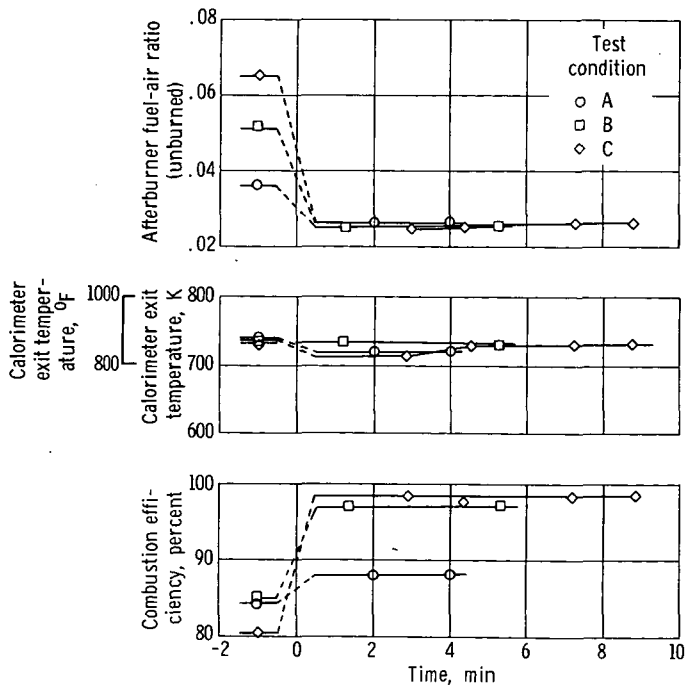


Figure 23. - Response of apparatus to a step change in afterburner fuel-air ratio.



NASA-Langley, 1973 —— 33 E-7262

NATIONAL AERONAUTICS AND SPACE ADMINISTRATION
WASHINGTON, D.C. 20546

OFFICIAL BUSINESS
PENALTY FOR PRIVATE USE $300

SPECIAL FOURTH-CLASS RATE BOOK

POSTAGE AND FEES PAID
NATIONAL AERONAUTICS AND SPACE ADMINISTRATION
451

U.S.MAIL

POSTMASTER: If Undeliverable (Section 158 Postal Manual) Do Not Return

*"The aeronautical and space activities of the United States shall be conducted so as to contribute . . . to the expansion of human knowledge of phenomena in the atmosphere and space. The Administration shall provide for the widest practicable and appropriate dissemination of information concerning its activities and the results thereof."*

—NATIONAL AERONAUTICS AND SPACE ACT OF 1958

# NASA SCIENTIFIC AND TECHNICAL PUBLICATIONS

TECHNICAL REPORTS: Scientific and technical information considered important, complete, and a lasting contribution to existing knowledge.

TECHNICAL NOTES: Information less broad in scope but nevertheless of importance as a contribution to existing knowledge.

TECHNICAL MEMORANDUMS: Information receiving limited distribution because of preliminary data, security classification, or other reasons. Also includes conference proceedings with either limited or unlimited distribution.

CONTRACTOR REPORTS: Scientific and technical information generated under a NASA contract or grant and considered an important contribution to existing knowledge.

TECHNICAL TRANSLATIONS: Information published in a foreign language considered to merit NASA distribution in English.

SPECIAL PUBLICATIONS: Information derived from or of value to NASA activities. Publications include final reports of major projects, monographs, data compilations, handbooks, sourcebooks, and special bibliographies.

TECHNOLOGY UTILIZATION PUBLICATIONS: Information on technology used by NASA that may be of particular interest in commercial and other non-aerospace applications. Publications include Tech Briefs, Technology Utilization Reports and Technology Surveys.

***Details on the availability of these publications may be obtained from:***

**SCIENTIFIC AND TECHNICAL INFORMATION OFFICE**

**NATIONAL AERONAUTICS AND SPACE ADMINISTRATION**

**Washington, D.C. 20546**